PERGAMON

Quaternary Science Reviews 20 (2001) 1561–1576

QSR

Millennial scale climate variability of the northeast Pacific Ocean and northwest North America based on radiolaria and pollen

N.G. Pisias[a,*], A.C. Mix[a], L. Heusser[b]

[a] College of Oceanic and Atmospheric Sciences, Oregon State University, 104 Ocean Administration Building, Corvallis, OR 97331, USA
[b] Lamont Doherty Earth Observatory, Palisades, NY, USA

Abstract

Radiolaria and pollen abundances in marine sediment cores from the northeast Pacific are used to reconstruct oceanographic and continental climate change during the past glacial cycle (0–150 kyr). These data allow direct comparison of the climate response of continental and oceanic systems. Detailed $\delta^{18}O$ and AMS-^{14}C measurements provide a link into global stratigraphic frameworks. Canonical correlation analysis extracts two modes of variation common to both the Radiolaria and pollen records. The first mode of variation correlates an assemblage of Radiolaria associated with coastal upwelling with increased redwood, western hemlock, and alder pollen. This association is consistent with the modern relationship between coastal upwelling, coastal fog and redwood forests. A second canonical mode relates an oceanic fauna now found in highest abundance in the far North Pacific with reduced pine and western hemlock pollen abundance.

Comparison of these records to an ice core $\delta^{18}O$ record suggests that at wavelengths >3000 years, warm events in Greenland are correlated to intervals of increased coastal upwelling off Oregon, decreases in importance of very cold North Pacific fauna (suggesting warming), and increases in pollen associated with wetter coastal environments. Radiolarian based sea-surface temperature estimates suggest that the variability of the northeast Pacific on this time scale is about 2°C. Warming in the coastal regions reflects reduced advection of the California Current, but is moderated by increases in cool coastal upwelling. We infer that the response of the northeast Pacific to millennial scale climate changes is related to changes in atmospheric circulation at mid- to high latitudes.

Preliminary analysis suggests that oceanic variability off Oregon at wavelengths <3000 years is similar to the Dansgaard–Oeschger cycles of the ice core $\delta^{18}O$ records. This variability is associated with changes in subtropical faunal elements without similar changes in other faunal elements. This finding suggests that, unlike longer-period millennial scale events, the propagation of the shorter wavelength events to the Northeast Pacific is through subtropical or tropical teleconnections.

1. Introduction

A major goal in the study of past climate change is to link ocean circulation change and climate change in continental regions. Achieving this goal depends on the ability to correlate oceanic and continental climate change records accurately. Here, we overcome correlation difficulties by measuring marine and continental climate tracers in the same marine sediment cores. Our inferences of oceanographic change are based on the relative abundance changes of radiolarian microfossils, while inferences about the history of continental climates are based on the relative abundances of pollen preserved in the same sample set used for marine microfossil analysis. Our records span the last full glacial cycle (150,000 years) and document millennial-scale variability in the Northeast Pacific and the northwestern United States.

2. Study region

2.1. Ocean climate and biota

The northeastern Pacific can be divided into three major oceanographic regions; the California Current, the Transition Zone, and the Alaskan Gyre. These three regions are influenced by continental runoff, upwelling, and by the North Pacific West Wind Drift current. The West Wind Drift, an eastward flowing surface current

*Corresponding author. Tel.: +1-541-737-5213; fax: +1-541-737-2064.
E-mail address: pisias@oce.orst.edu (N.G. Pisias).

0277-3791/01/$ - see front matter
PII: S0277-3791(01)00018-X

forms the northern limb of the North Pacific subtropical gyre and crosses the Pacific between approximately 40° and 45°N latitudes (~13°C isotherm in Fig. 1a). Its northern edge defines the Subarctic Front (Roden, 1975). The subpolar Alaskan Gyre, defined by a cyclonic (counterclockwise) circulation, lies north of the West Wind Drift. The West Wind Drift meets the coast of North America in a "Transition Zone" which marks the boundary between the southward flowing California Current and the northward flowing Alaskan Stream near the coast of North America. The California Current defines the eastern boundary of the anti-cyclonic (clockwise) North Pacific subtropical gyre. The Alaskan Stream defines the eastern and northern boundaries of the Alaskan Gyre (Fig. 1a).

The region between 40° and 45°N latitude has a significant seasonal cycle in surface winds (Huyer, 1983). This cycle is driven by the seasonal migration of the North Pacific high-pressure cell and is associated with a strong seasonal cycle in coastal upwelling in northern parts of the California Current. During the winter the North Pacific high-pressure cell is displaced southward by the Aleutian low-pressure cell which results in predominately on-shore winds from the southwest along the Oregon and Washington Coasts. In summer the Aleutian low moves northward and is replaced by the North Pacific high so that surface winds come from the north all along the California Current.

Two oceanic processes observed in the California Current are coastal and open-ocean upwelling. Offshore Ekman transport due to northerly winds produce upwelling of cold and nutrient-rich waters near the coast. The coastal upwelling off Oregon is a relatively weak seasonal phenomenon compared to that off Northern California, which is strong year-around (Huyer, 1983). In the open ocean, Ekman pumping, driven by cross-current gradients in windstress, called windstress curl, is observed in the main stream of the California Current and in the Alaskan Gyre (Bakun and Nelson, 1991). By convention, positive windstress curl forces open-ocean upwelling, while negative windstress curl forces downwelling. In winter, windstress curl is positive off shore from southern Oregon to southern California. South of 40°N positive windstress curl continues through the summer. Thus, within the region influenced by coastal upwelling, windstress curl induced open-ocean upwelling is present year around. Both upwelling processes are associated with increased productivity, but each process has a distinct faunal response (Ortiz et al., 1997). Coastal upwelling is characterized by blooms of larger diatoms and is associated with high export productivity (Hood et al., 1994) whereas open-ocean upwelling is often associated with small phytoplankton and has relatively low export productivity due to high grazing pressure and intense nutrient recycling (Miller et al., 1991).

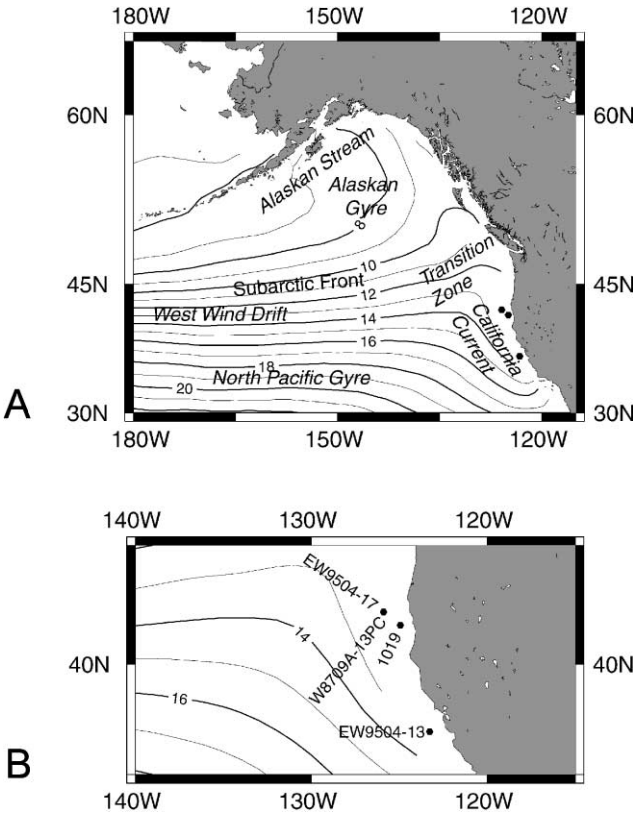

Fig. 1. (A) Study location map showing general circulation features of the North Pacific. Contours show mean annual surface ocean temperatures from Levitus (1982), large dots off the west coast of North America show location of sediment cores used in this study. (B) Close-up of core locations with annual mean sea surface temperatures as shown in A.

Radiolarian assemblages are used here to evaluate changes in surface ocean conditions in the eastern North Pacific. Seven assemblages were identified from a Q-mode factor analysis of 170 Pacific Ocean sea-floor sediment samples from tops of gravity and piston cores (Pisias et al., 1997). Four assemblages that are important in the Northeast Pacific during the late Pleistocene are shown in Fig. 2. The "Transitional" assemblage is associated with water masses in the transition zone of the California Current and Alaskan Gyre where open-ocean wind-driven upwelling dominates (Fig. 2a). The primary radiolarian species associated with this assemblage are *Botryostrobus aquilonaris*, *Lithelius minor*, and *Echinomma delicatum*. The "Eastern Boundary Current" (EBC) assemblage is associated with coastal upwelling in eastern boundary currents of the Pacific, especially off Mexico and Peru (Fig. 2b). Species important in this assemblage include *C. davisiana davisiana*, *Pterocorys minithorax*, *Pterocorys clausus* and *Pterocorys zancleus*. The "Bering Sea" assemblage predominates in the cold waters of the subpolar North Pacific (Fig. 2c). In modern surface sediments this assemblage is rare or absent off Oregon

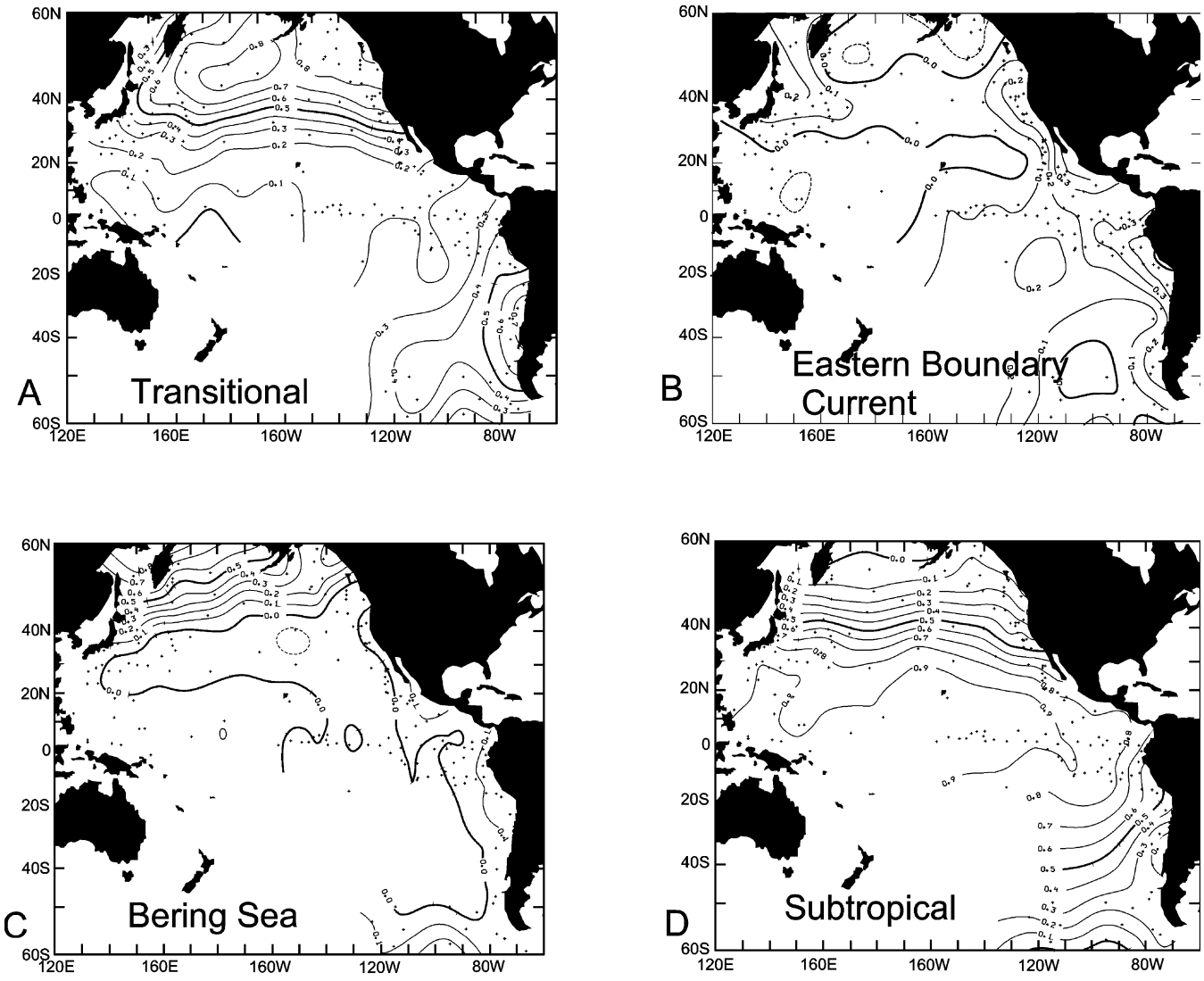

Fig. 2. Factor loadings of radiolarian assemblages determined from a Q-mode factor analysis (Imbrie and Kipp, 1973) of radiolarian census data from core-top sediments of the Pacific (Sabin and Pisias, 1996; Pisias et al., 1997). (a) Distribution of radiolarian assemblage associated with the transition zone of the North Pacific; (b) assemblage associated with the upwelling of the Eastern Boundary Current and; (c) assemblage associated with the very cold surface ocean conditions of the far North Pacific and Bering Sea.

and California, but it is important here during glacial intervals. The most important species of this assemblage is *Ceratospyris borealis*. The "subtropical" assemblage found in the eastern North Pacific is now abundant in the tropical and subtropical regions of the Pacific (Fig. 2d). In the Northeast Pacific two key species of this group, *Tetrapyle octacantha* and *Octopyle stenozona,* are more abundant in sediment trap samples from the warmer offshore waters of the northeast Pacific, than in the core of the California Current (Welling et al., 1992). During the last glacial interval this assemblage was a minor component of the radiolarian population all along the western margin of the eastern North Pacific (Sabin and Pisias, 1996). In Holocene sediments off the coast of southern California, increase abundance of a similar assemblage were used to infer stronger transport in the northward flowing coastal countercurrent during the past 8000 years (Pisias, 1978).

2.2. Terrestrial climate and vegetation

Topography as well as atmospheric circulation, control the cool, equable climates of coastal California and Oregon, a region associated with high precipitation and low evaporation. In summer, inland warmth turns zonal circulation southward along the coast. As eastward moving air is forced to rise, precipitation increases at a rapid rate on the seaward slopes of the Coast Range. Cool sea-surface temperatures associated with nearshore upwelling create fog, which keeps coastal climates cool in the summer (Barbour and Major, 1977; Barbour and Billings, 1988). Mean annual surface-air

temperatures and precipitation range from ~17°C and ~80 cm on the Northern California coast to ~12°C and ~300 cm in Oregon (Elford, 1974).

The natural coastal vegetation of northern California and Oregon is the southern extension of the moist coniferous lowland forests characterized by western hemlock (*Tsuga heterophylla*) and spruce (*Picea sitchensis*). This flora extends north to Alaska (Fig. 3a). The magnificent coastal redwoods (*Sequoia sempervirens*), which distinguish the California lowland forest, occur along a narrow (~20 km) fog-bound strip from southern Oregon to central California (Fig. 3f). Away from the moderating effects of the ocean and fog, in the warmer and drier interior a mosaic of oak woodlands and grassland is found. This mosaic is replaced at high altitudes by montane and subalpine forests of fir (*Abies concolor* and *Abies amabilis*), pine (*Pinus ponderosa* and *Pinus lambertiana*), and mountain hemlock (*Tsuga mertensiana*). Deciduous hardwoods are not common in Pacific Northwest forests except on riparian and disturbed sites where alder (*Alnus*) is prominent.

Pollen in marine sediments reflects the composition of the major natural coastal plant associations onshore, somewhat modified by fluvio-marine sedimentation processes (Fig. 3). Western hemlock, spruce, and alder, important components of the temperate coastal rainforest, are reflected in the abundance of pollen deposited offshore. Pollen from these species is concentrated off the areas of maximum development of the lowland Pacific coastal forest from Oregon to British Columbia. Redwood and oak pollen are prominent in the southern part of the study area, reflecting the importance of these species on the northern California coast (Fig. 3). Note that the distribution of redwood pollen is basically restricted to the distribution of coastal redwood forests onshore, an ecotone between southern oak woodlands and northern conifer forests. In cores taken south of 36°N, oak-herb-chaparral pollen reflects the arid oak woodland and open scrub of southern California. The distribution of pine pollen in northeast Pacific marine sediments reflects relative over-representation of pine because of its hydrodynamic efficiency.

3. Samples and methods

Table 1 gives the locations and sampling data for the sediment cores used in this study (Fig. 1b). For the first three core sites listed in Table 1, pollen and radiolarian analyses were completed on splits of the same samples. A few additional radiolarian samples from core W8709A-13PC were analyzed for a more complete characterization of the Younger Dryas interval. Separate sample sets were used from ODP Site 1019. Most the pollen and radiolarian samples were taken from hole 1019C.

Radiolaria microscope slides were prepared following the technique of Roelofs and Pisias (1986). Species census data use the same taxonomic groups of Pisias et al. (1997) and are expressed here in terms of assemblages identified from a set of 170 Pacific Ocean surface sediment samples (Pisias et al., 1997). At least 500 specimens were counted in each sample. Species percentages $>1\%$ are significantly different from zero. Percentages of 20% have uncertainties of ± 4 (1 standard deviation; Cochran, 1963).

Estimates of mean annual sea-surface temperatures were based on the transfer function of Pisias et al. (1997). The transfer function was developed using the technique of Imbrie and Kipp (1971). Unlike previous radiolarian based transfer functions, the census percentage data were first transformed with a logarithmic transformation. This transformation is used to make percentage data more normally distributed and to give more weight to the rarer species than a purely linear transformation. The transfer function thus, assumes that the species percentage data for Radiolaria respond non-linearly to changes in ocean temperature. The standard error of estimate for mean annual SST estimates is 1.6°C. Radiolarian and alkenone estimated temperatures in nearby core W8709A-8PC agree within their statistical errors (Prahl et al., 1995). This paleotemperature equation was used by Sabin and Pisias (1996) to study the deglacial history of the California Current.

Pollen slides were prepared following the technique of Heusser and Stock (1984). Pollen types were identified to the finest taxonomic level possible; for example, specific identification of *Tsuga* (*T. heterophylla* and *T. mertensiana*), and the papillate thick/exined grains of *Sequoia sempervirens*. Inaperturate pollen of taxa in the Taxodiaceae, Cupressaceae, and Taxaceae (e.g., *Juniperus, Torreya, Cupressus, Libocedrus, Chamaecyparis,* and *Thuja*) that are not satisfactorily separated using light microscopy were grouped as "TCT" (taxonomic nomenclature follows Munz, 1968; Hitchcock and Cronquist, 1973). Other groups of pollen include members of the Anacardiaceae, Rhamnaceae and Rosaceae), and families of herbs (Gramineae, Cyperaceae, and Compositae). At least 300 specimens were counted in each sample. Species percentages $>2\%$ are significantly different from zero. Percentages of 20% have uncertainties of ± 5 (1 standard deviation; Cochran, 1963).

4. Results and discussion

4.1. Surface ocean

A well-dated detailed record of the last deglacial transition for the northern region of the California

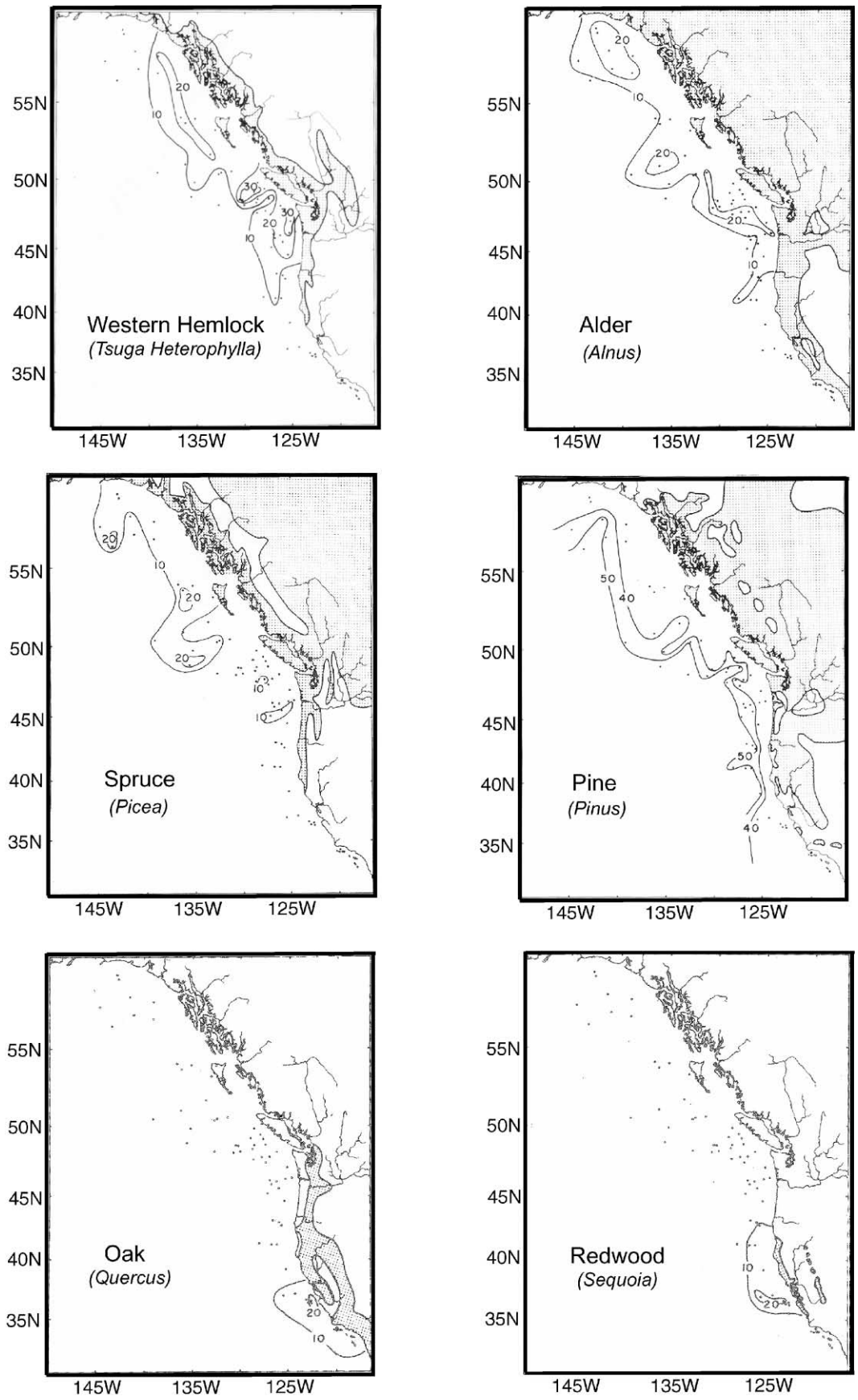

Fig. 3. Pollen distribution in surface sediments of the eastern North Pacific (from Heusser and Balsam, 1977).

Table 1
Piston cores

Core ID	Latitude (°N)	Longitude (°W)	Water depth (m)	Average sampling interval cm (years)
EW9504-17PC	42.24	125.89	2671	5 (470)
EW9504-13PC	36.99	123.27	2510	5 (220)
ODP Site 1019	41.68	124.93	989	15 (280)
W8709A-13PC	42.12	125.75	2712	13 (650)

Current is provided by core W8709A-13PC (Fig. 4). Twenty AMS-^{14}C age dates are available over the interval from 7000 to 25,000 cal-years BP (down-pointing arrows in Fig. 4, Table 2; chronology from Mix et al., 1999; all ages are calendar corrected based on CALIB4 and the INTCAL-98 calibration, Stuiver et al., 1998). Shown with the Radiolaria data is the GISP2 δ^{18}O record (Stuiver and Grootes, 2000). The GISP2 δ^{18}O record, (dashed green) is shown in this and subsequent figures as a reference for millennial scale variability.

Variations in surface ocean conditions in core W8709A-13PC can be inferred from the Subtropical, Transitional, EBC and Bering Sea radiolarian assemblages. Also shown are transfer function estimates of mean annual SST for this core.

The overall deglacial record shown in this core is typical for much of the region (Sabin and Pisias, 1996). During full glacial conditions ($\sim$20,000 cal-years BP) the radiolarian fauna is dominated by the Bering Sea assemblage (Fig. 2c). The abundance of species associated with coastal upwelling in the eastern boundary currents, the EBC assemblage (Fig. 2b), is significantly reduced relative to modern conditions.

The deglaciation is marked by a decrease in the abundance of the Bering Sea assemblage (implying warming) followed by a later increase in the abundance of Transitional and EBC assemblages (Fig. 4). During the Younger Dryas interval (13,000–11,500 cal-years BP), the Bering Sea assemblage does not return to full glacial abundances, but the EBC assemblage is replaced by the Transitional species, suggesting a reduction in coastal upwelling.

The estimated sea-surface temperatures do not show a simple deglacial warming trend in core W8709A-13PC. The very cold conditions suggested by the Bering Sea assemblage are replaced by conditions of enhanced coastal upwelling associated with the EBC assemblage. Both of these processes maintain cool surface conditions but through different causes. These results are consistent with Ortiz et al. (1997) who inferred low coastal upwelling and expanded influence of the Alaska Gyre during the Last Glacial Maximum (LGM). These results also agree with the inference of strongest coastal upwelling during the Allerod-Bolling (14,500–13,000

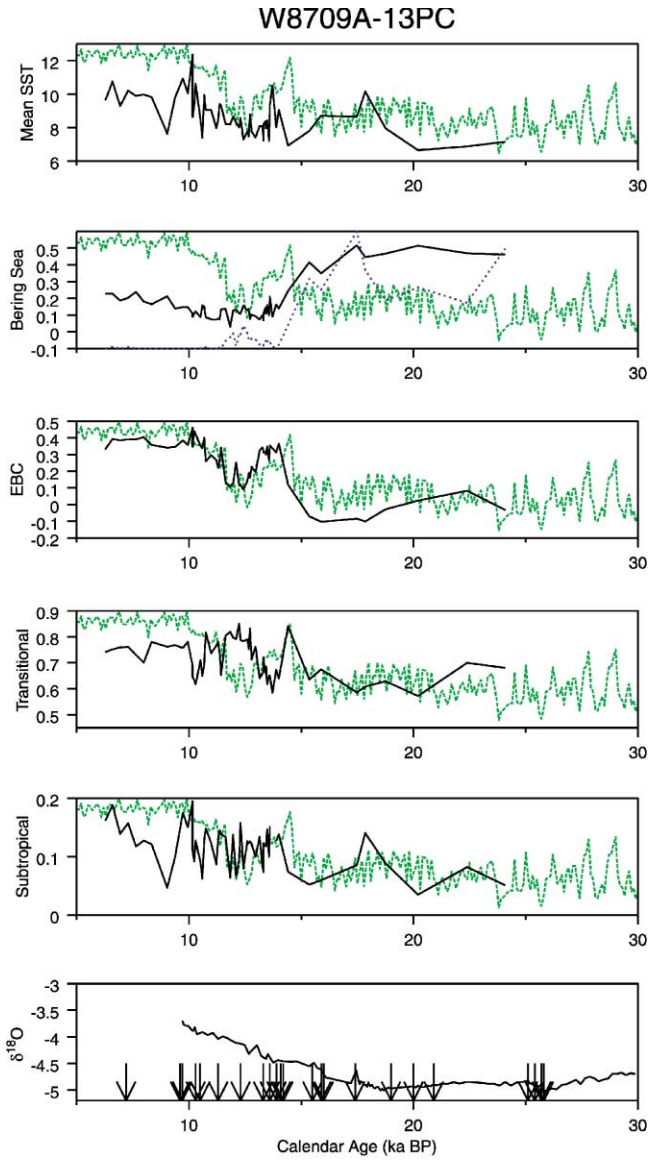

Fig. 4. Time series records (5000 to 30,000 cal-years BP) of radiolarian assemblages and estimates mean annual sea surface temperatures for core W8709A-13PC. Down pointing arrows indicate position of 20 ^{14}C AMS dates available for this core (Mix et al., 1999). Green curve in each frame is the GISP2 ice core δ^{18}O record from Stuiver and Grootes (2000) and is shown for reference to magnitude and wavelength of climate variability during the past 60 ka. Blue dotted line plotted with Bering Sea fauna is the relative abundance of species *Ceratospyris borealis* the dominant species of this assemblage.

Table 2
Chronologies (calendar ages)

W8709A-13PC[a]		ODP Site 1019[a]		EW9504-13PC[b]		EW9504-17PC[b]	
Depth (cm)	Age (kyr)	Depth (cm)	Age (kyr)	Depth (cm)	Age (kyr)	Depth (cm)	Age (kyr)
27.50	7.2	284	6.8	0	12.0	0.0	0.0
96.25	9.6	417	10.1	130	16.5	96.0	7.5
98.75	9.7	492	10.6	430	24.8	386.0	18.0
126.25	10.3	516	11.2	530	30.4	826.0	57.0
128.75	10.5	581	12.7	570	36.0	1046.0	81.5
139.00	11.3	621	13.0	770	43.0	1350.0	122.0
154.00	12.3	711	14.8	930	50.0	1441.0	128.0
170.50	13.3	821	17.0	1100	66.0	1500.0	140.0
181.00	13.6	954	18.1	1400	73.0		
191.50	13.9	1055	21.0				
196.25	14.1	1215	24.0				
198.75	14.2						
212.50	15.5						
221.25	15.9						
223.75	16.0						
227.50	17.4						
301.25	19.0						
303.75	20.0						
332.50	20.9						
382.00	25.1						
392.50	25.4						
401.25	25.7						
403.75	25.8						
497.00	32.1						
557.00	36.4						

[a] Age model determined from calendar corrected AMS ^{14}C from Mix et al., 1999.
[b] Age model determined by correlation of benthic foraminifera $\delta^{18}O$ to W8709A-13PC.

cal-years BP) and early Holocene (11,000–8000 cal-years BP) intervals (Mix et al., 1999).

In Figs. 5–7, we show oceanographic records spanning the last 60 ky in three cores from the northern California Current. Chronologies at cores W8709A-13PC and ODP Site 1019 are from Mix et al. (1999). Note that uncertainty in the age models increases beyond 24,000 cal-years BP because calendar corrections cannot be applied to radiocarbon dates with certainty. A deglacial pattern of change in radiolarian fauna roughly similar to that of W8709A-13PC occurs at all three sites, although the southern-most site (EW9504-13PC; Fig. 5) reveals a systematic glacial to interglacial warming of about 4°C.

At the nearshore site, near the Oregon–California border (ODP Site 1019; Fig. 6), the cold water Bering Sea assemblage has a small maximum and the Transitional assemblages show a significant maximum during the Younger Dryas. The small maximum in the cold water Bering Sea assemblage is not observed at the offshore sites (e.g., EW9504-17PC, Fig. 7) or to the south (EW9504-13PC; Fig. 5). Unlike foraminiferal evidence based on the coiling direction of *Neoglobaquadrina pachyderma,* which suggests that the Younger Dryas is characterized by near glacial conditions (Mix et al., 1999), the Radiolaria data suggest that the LGM and Younger Dryas intervals are oceanographically different. The Radiolaria and foraminifera data both indicate reduced coastal upwelling during the Younger Dryas interval, but the Radiolaria suggest a greater influence of the transitional water masses without a return to Bering Sea conditions during the Younger Dryas.

During glacial times the species *Ceratospyris borealis* represents on an average 12–15% of the radiolarian population found in core EW9504-7PC (abundance curves for this species are shown as blue dotted lines in Figs. 4, 6 and 7 with Bering Sea assemblage). In surface sediments, abundance estimates this high are found only in surface sediments of the far North Pacific and Bering Sea (data from Pisias et al., 1997). In core EW9504-17PC the abundance of *C. borealis* begins to decrease rapidly at 14.3 ka and disappears from this site between 11.6 and 11.8 ka (Fig. 7) and in core W8709A-13PC *C. borealis* disappears between 11.4 and 12.1 ka (Fig. 4). The Younger Dryas is recorded in sites off Oregon and Northern California as a decrease in the importance of the EBC assemblages and an increase in the importance of the Transitional assemblage (sites EW9504-17PC and 1019; Figs. 6 and 7) while off Central California there is

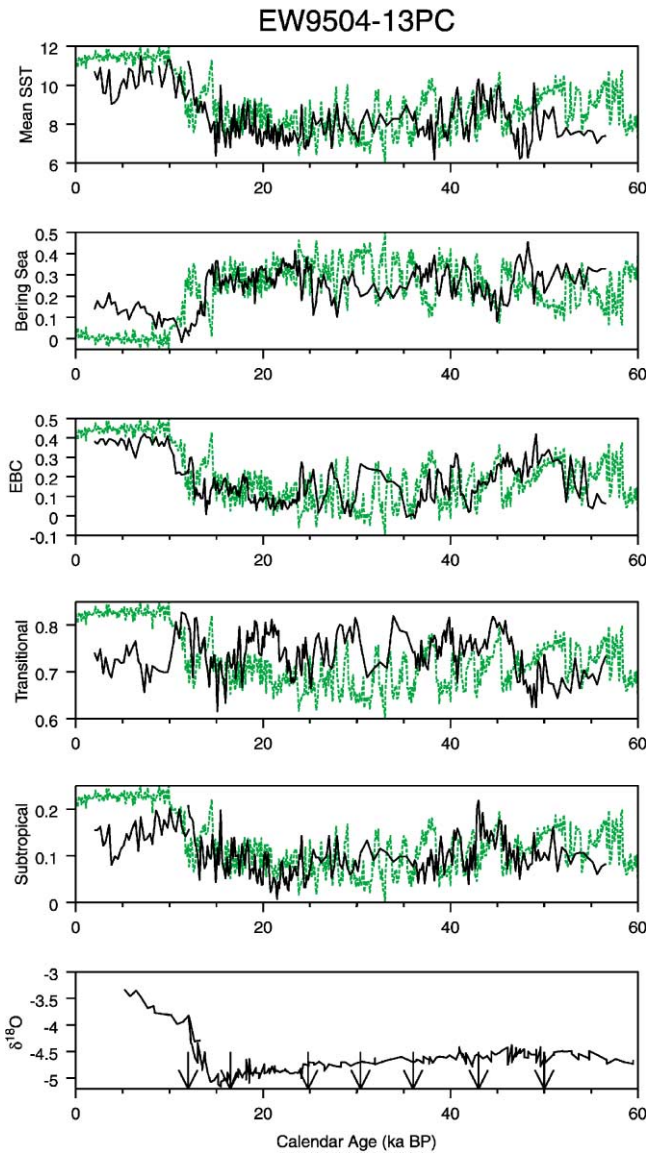

Fig. 5. Time series records of radiolarian assemblages and estimates mean annual sea surface temperatures for core EW9504-13PC. Down pointing arrows indicate position of age control points listed in Table 2. Green curve as in Fig. 4.

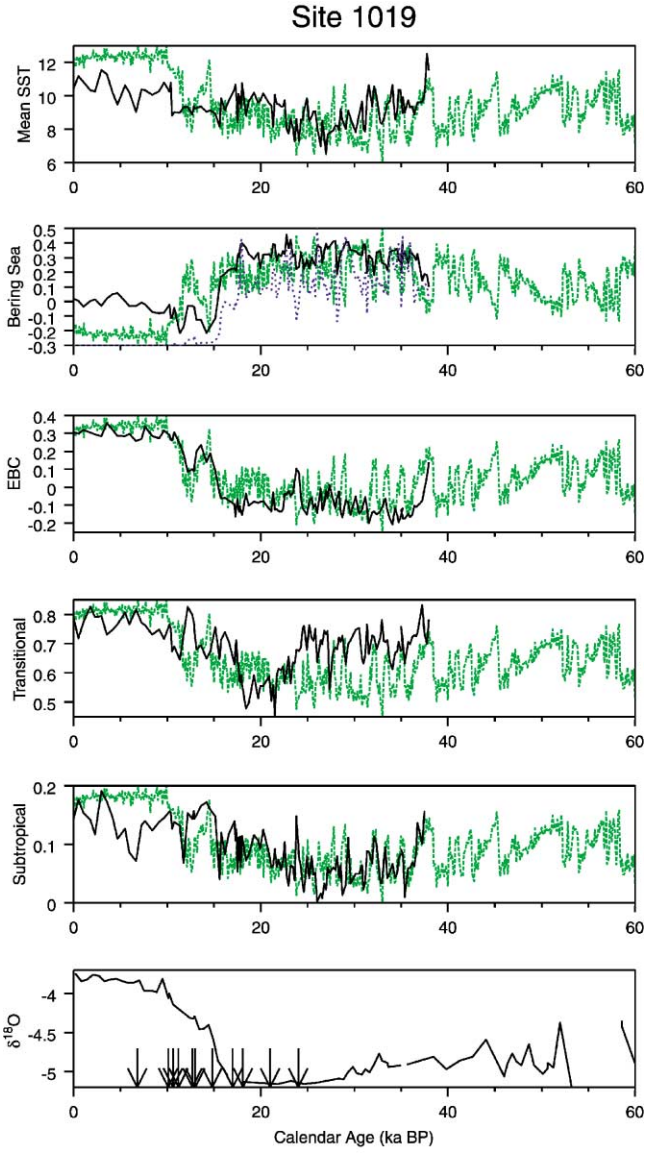

Fig. 6. Time series records of radiolarian assemblages and estimates mean annual sea surface temperatures for Ocean Drilling Program Site 1019. Blue dotted line plotted with Bering Sea fauna is the relative abundance of species *Ceratospyris borealis* the dominant species of this assemblage. Down pointing arrows indicate position of age control points listed in Table 2. Green curve as in Fig. 4.

very little radiolarian faunal response to the Younger Dryas event (site EW9504-13PC; Fig. 5).

One of the key oceanic responses to millennial climate variability recorded by the radiolarian fauna is a change in coastal upwelling. We can evaluate the magnitude of oceanographic change represented by these records using the results of a regional scale climate model. Fig. 8 shows coastal upwelling along the west coast of North America calculated from the National Center for Atmospheric Research (NCAR) atmospheric regional climate model (RegCM). This regional model was forced by four different runs of the T31 version of the GENESIS model (Hostetler et al., 1999). The control run is for modern boundary conditions generated by GENESIS. The LGM is represented by model run MaxCold (maximum ice volume and cold North Atlantic SST based on the LGM of CLIMAP, 1981). The other model runs in Fig. 8 represent different stages of a "canonical" Heinrich event, MinCold is reduced Laurentide ice sheet volume and a cold North Atlantic, and MinWarm is reduced Laurentide ice sheet volume and warmer North Atlantic (half way between modern and LGM SST values).

In the MaxCold run, coastal upwelling decreases in January and July relative to the control run. This change is consistent with the radiolarian data and with

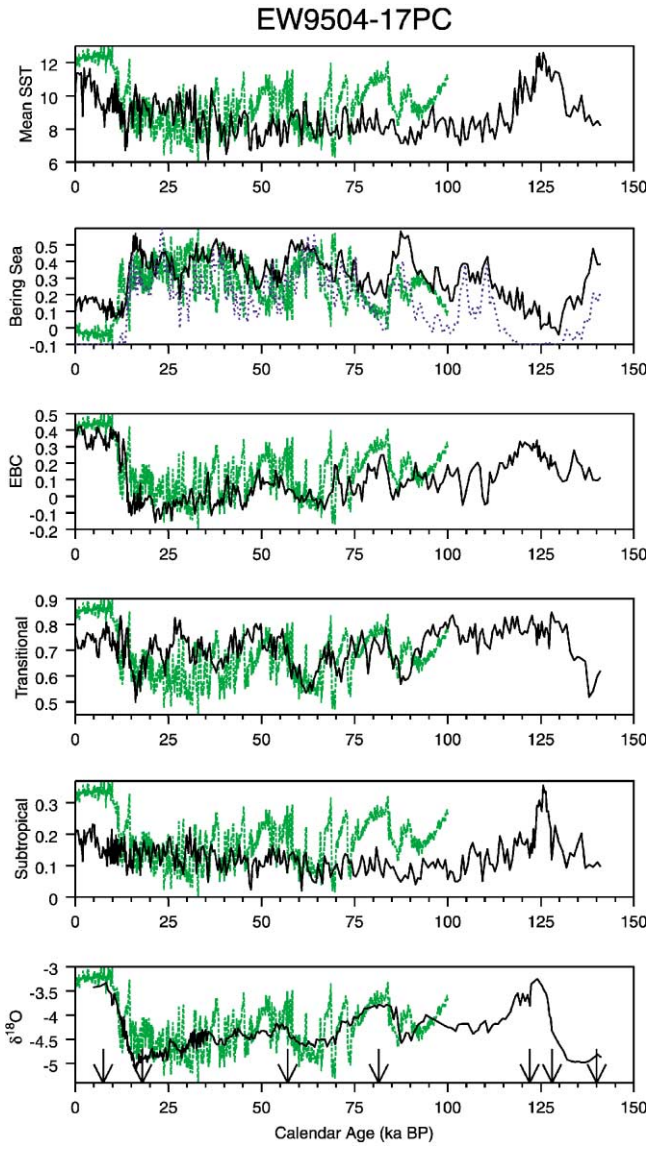

Fig. 7. Time series records of radiolarian assemblages and estimates mean annual sea surface temperatures for core EW9504-17PC. Down pointing arrows indicate position of age control points listed in Table 2. Blue dotted line plotted with Bering Sea fauna is the relative abundance of species *Ceratospyris borealis* the dominant species of this assemblage. Green curve as in Fig. 4.

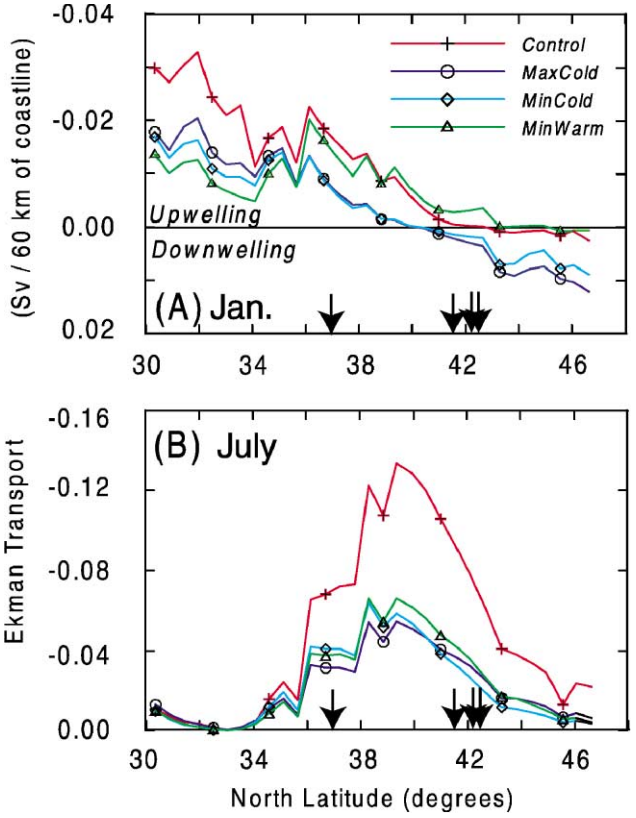

Fig. 8. Offshore Ekman transport (i.e., coastal upwelling) along the west coast of North America calculated from a regional scale climate model. The regional model was imbedded into four different runs of the T31 version of the GENESIS model (see Hostetler et al., 1999). Down pointing arrows show latitudinal position for cores used in this study.

inferences based on foraminiferal and organic carbon data for reduced productivity at the glacial maximum (Ortiz et al., 1995; Mix et al., 1999). The MaxCold model run predicts approximately 50% decrease in July upwelling at the core sites. In January, coastal upwelling decreases at the southern sites, while downwelling occurs at the northern sites.

Among the core sites, the magnitude of change in the model coastal upwelling from modern to full glacial conditions is proportional to the magnitude of change in the radiolarian EBC assemblage. For example at the southern site, EW9504-13PC, the model predicts a change in offshore transport of 0.04 Sv/60 km between modern and the glacial maximum. (Note that Sv is a Sverdrup or water transport of $10^6\,m^3/s$. Thus, Sv/60 km is $10^6\,m^3/s$ transport per 60 km of coast line. Transport is calculated normal to coast and by convention, positive is eastward and negative is westward away from the coast.) Here we observe a change in the radiolarian EBC fauna of 0.3. At the northern sites the model predicts a change in Ekman transport of 0.05 Sv/60 km. This corresponds to a faunal change of 0.45. The ratio of change in transport to change in the EBC fauna are 0.13 and 0.11 for these two locations.

The upwelling response predicted by the model for the "canonical" Heinrich event is very small (Fig. 8). However, the EBC fauna varies within the glacial interval by 60% of the glacial/interglacial change in the southern site and about 40% in the northern sites. This suggests that the model runs, forced only by changes in glacial ice volume and changes in SST's of the North Atlantic, are missing key local changes in important boundary conditions that would affect alongshore winds.

Sea-surface temperature estimates indicate that millennial scale temperature variability is of the order of

2°C in the Northeast Pacific, small but greater than the standard error of the regression estimates. However, the relationship between temperature and faunal changes is not straightforward. For example, we do not see a significant Younger Dryas response in sea-surface temperatures, and in the northern-most sites, we also do not see a simple glacial/interglacial response of SST even though we see important faunal changes. The increase in coastal upwelling during "warm" events may act as a negative feedback, keeping sea-surface temperatures cool. This appears to be the case in the northern-most sites during the deglacial transition and into the interglacial interval. However, glacial to interglacial warming is significant at the southern-most core site, EW9504-13PC. This is driven by glacial to interglacial increase in the subtropical assemblage in this core (Fig. 5). The northern cores do not record a similar change in this assemblage at this time. At site EW9504-13PC, where we see similar but opposite changes in the subtropical and the other dominant fauna, the changes in the subtropical assemblage may reflect the influence of waters transported northward by coastal counter-currents and/or a generally weaker flow of the California Current allowing more subtropical waters into the region of Central California.

4.2. Terrestrial climates

Using the well-dated deglacial record of W8709-13PC we can link the Pacific Northwest pollen records into the marine stratigraphic record (Fig. 9). Here we show the relative abundance of 6 pollen types during the past 60 kyr. Details of the pollen record spanning the LGM to Holocene interval from this region are given by Heusser (1998). In general, the pollen records suggest that temperatures in the coastal regions of Oregon may have been 2°C to 3°C cooler than present during most of the last glacial interval, but that during the LGM temperatures may have been ~5°C cooler than present (Heusser, 1998). Precipitation in the coastal region of Northern California and Oregon is inferred to be slightly higher during the LGM than during the Holocene suggesting a steeper precipitation gradient inland where precipitation decreased (Whitlock and Grigg, 1999). The deglacial interval is marked by an early increase in alder, a species associated with colonization of recently disturbed ground or with reorganization of plant communities related directly or indirectly to climate change. Continued warming, indicated by a subsequent increase in oak pollen, is followed by conditions conducive for redwood forests (slightly lower summer temperatures related to enhanced summer fog associated with coastal upwelling).

Except for a resurgence of pine, the pollen sequences do not vary significantly during the Younger Dryas event as indicated by the GISP2 $\delta^{18}O$ data (Fig. 9). A brief expansion of spruce and pine (suggestive of lower temperatures) immediately precedes the Younger Dryas, as do glacier advances on Mt Rainier (Heine, 1998). In a pollen record from Little Lake in the Oregon coast range, Grigg and Whitlock (1998) note a similar response during the Younger Dryas. At this site there is a general increase in pine with a decrease in *Pseudotsuga* (Douglas fir), suggesting a "generally weak registration of a Younger Dryas ..." at Little Lake as compared to other sites in northwest North America (Grigg and Whitlock, 1998). They speculate that this might reflect the inland nature of their study sites and that locations near the coast, closer to direct influence of oceanic changes, might have a stronger Younger Dryas response.

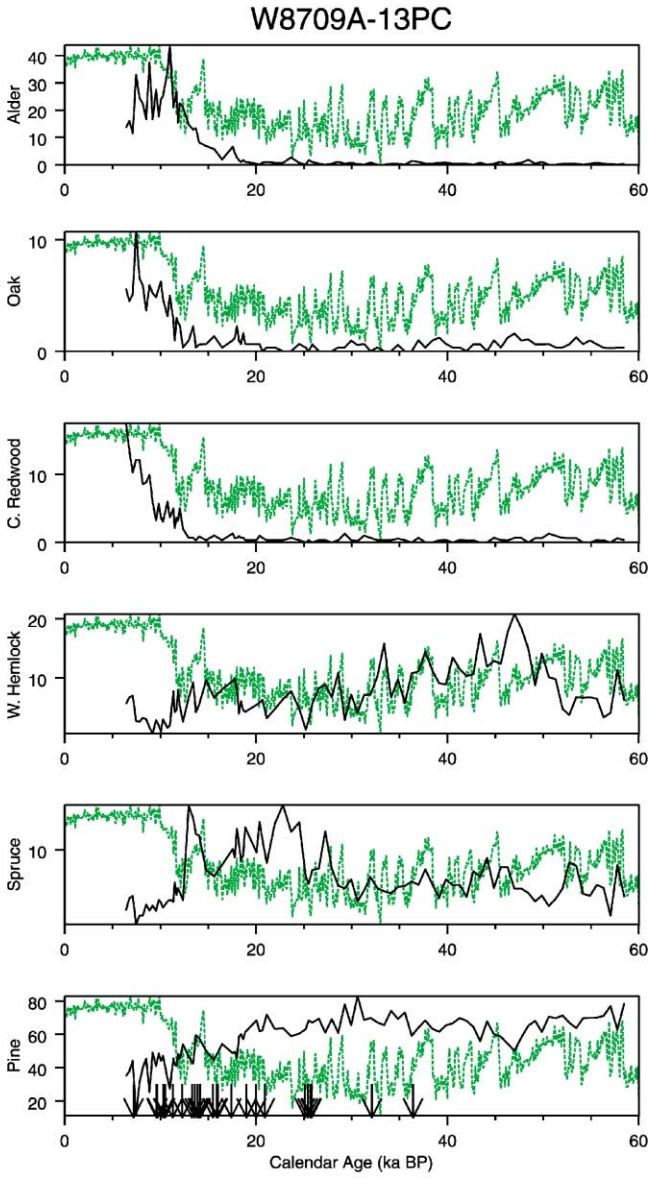

Fig. 9. Time series records of pollen abundance of selected pollen types for core W8709A-13PC. Green curve as in Fig. 4.

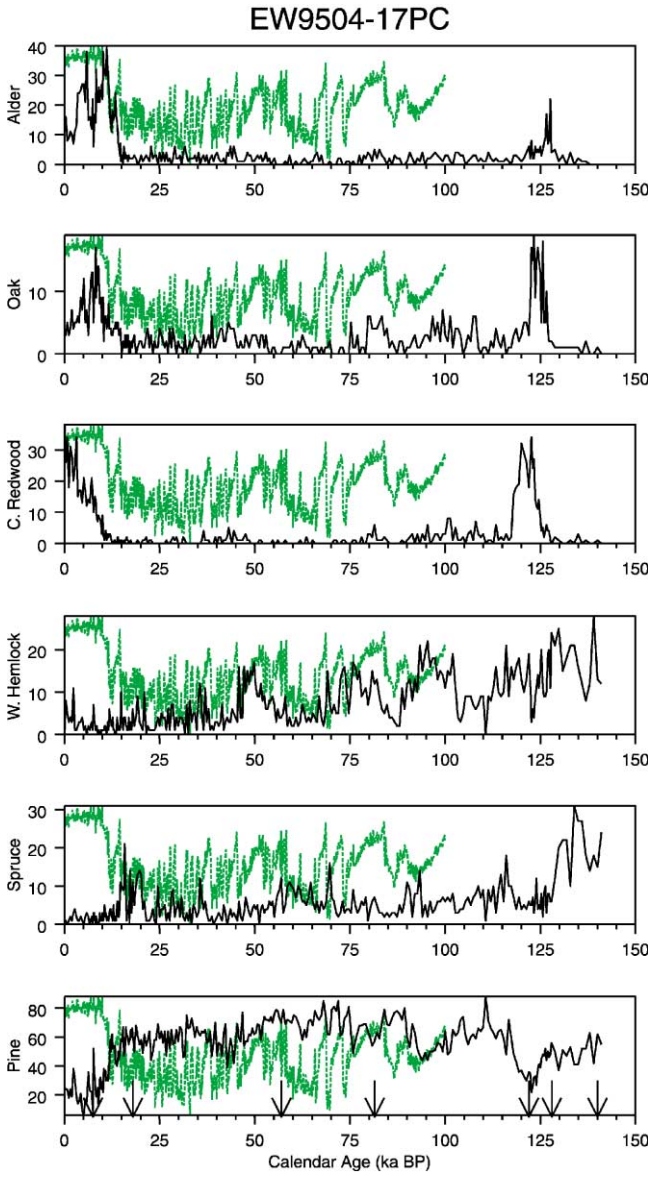

Fig. 10. Time series records of pollen abundance of selected pollen types for core EW9504-17PC. Green curve as in Fig. 4.

Pollen relative abundances from EW9504-17PC (Fig. 10) extend the high-resolution record of northwest Pacific coastal environments through the last interglacial interval (Heusser et al., 2000). Pollen assemblages from the last 60 ky in this core closely resemble those from nearby core W8709-13PC. The succession of alder, oak, and redwood that marks Holocene pollen data from core W8709-13PC is seen in two interglacial intervals (MIS 1 and 5e). Differences in the abundances of the oak pollen in these two events in EW9504-17 (Fig. 10) suggest that enhanced development of xeric oak woodland during the early part of the last interglacial period. This would suggest summers during the last interglacial interval were warmer and drier than summers of the present interglacial. The radiolarian data from EW9504-17PC also indicate that SST's during the last interglacial were warmer than present (Fig. 7). There are clear differences between the pollen assemblages that immediately precede each of the interglacial intervals. The greater amount of western hemlock (and spruce) in MIS 6 compared with MIS 2 implies that the open, pine-dominated woodland was more extensive during the last glacial maximum than during the glacial maximum represented by MIS 6.

4.3. Ocean continental linkages

We use canonical correlation to evaluate how oceanographic changes (as reflected in the radiolarian assemblages) are related to changing continental climates (as reflected in the pollen assemblage). Our goal is to extract the record of climate change that is common to the eastern North Pacific Ocean and western North America. The responses of the oceanic and continental ecosystems to climate change in this region reflect differing response times of processes associated with ocean circulation and temperature and processes of continental forest succession and ecosystems. But what is the common climate response of these systems?

In using canonical correlation we assume that some linear combination of the pollen species percentages represents a climate response. This assumption is supported by Whitlock and Bartlein (1997) who conclude that climate variations are the primary cause of regional vegetation change on millennial timescales. We assume that a linear combination of the radiolarian assemblages (that are in turn based on log-transformed species data) reflects the oceanic response. Canonical correlation defines the linear combination of pollen species that is most highly correlated with a linear combination of radiolarian assemblages. We can think of canonical correlation as a more complex form of multiple regression. In generating paleotemperature estimates, we use a linear combination of radiolarian assemblages that is most highly correlated to an independent variable set—sea surface temperature. In this case one data set (sea-surface temperatures) only has one variable rather than the multivariate sets represented here by pollen and radiolarian data. As in the case of paleotemperature transfer functions, we assume that the common variate is a measure of climate change.

In Figs. 11 and 12 the black line is the linear combination of radiolarian assemblages and the red line is the linear combination of the pollen species percentages. The green line is the GISP2 ice core $\delta^{18}O$ record. The correlation coefficient between pollen and radiolarian time series for the first variate is 0.91. This correlation is calculated over all samples from cores W8709A-13PC and EW9504-17PC with both radiolaria and pollen analysis. This canonical variate correlates a

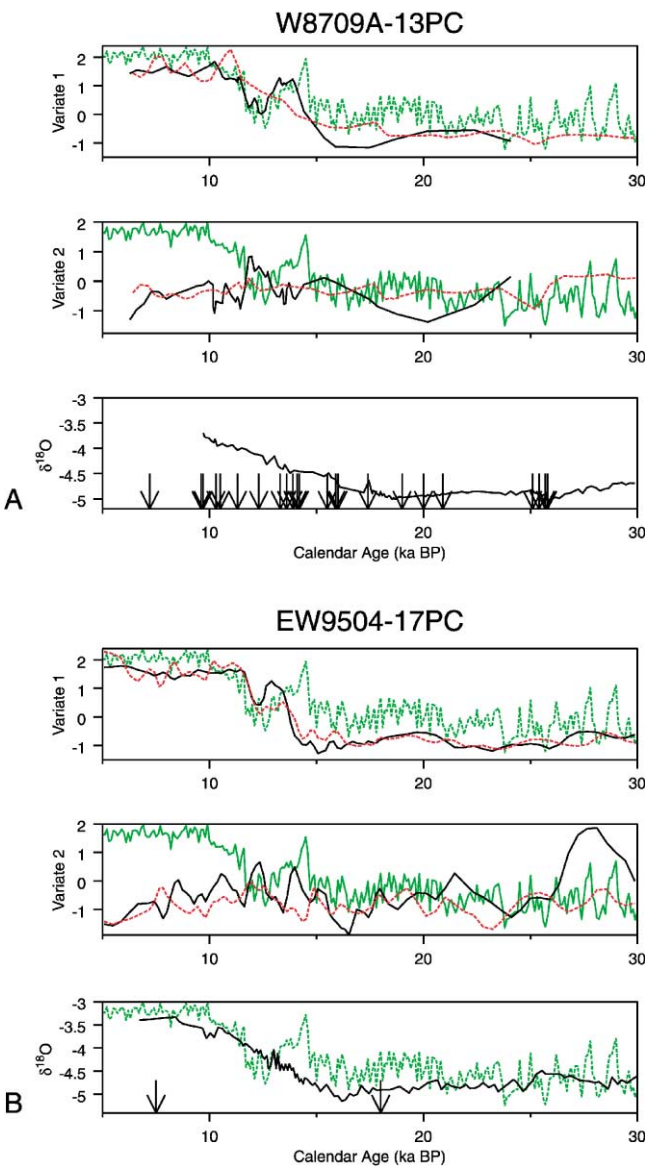

Fig. 11. Time series from 5000 to 30,000 cal-years BP for canonical variates determined from the multivariate pollen and radiolarian data sets. (a) variates determined for core W8709A-13PC; (b) variates for EW9504-17PC. Age control points from Table 2 shown as down pointing arrows. Black lines are the canonical variates for all Radiolaria samples and red lines are canonical variates calculated from pollen samples. Green curve as in Fig. 4.

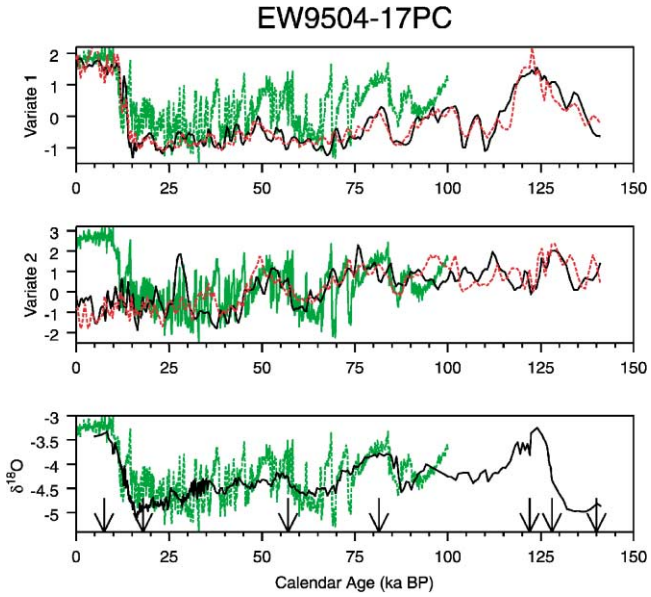

Fig. 12. Time series from 0 to 150,000 cal-years BP for canonical variates determined from the multivariate pollen and radiolarian data sets from core EW9504-17PC. Age control points from Table 2 shown as down pointing arrows. Black lines are the canonical variates for Radiolaria assemblages and red lines are canonical variates calculated from pollen samples. Green curve as in Fig. 4.

Table 3
Canonical coefficients

Radiolaria	Weight	Weight	Pollen
Canonical variate 1			
Subtropical	0.043	0.153	Pine
Transitional	−0.100	0.140	Spruce
EBC	0.494	0.306	Western Hemlock
Bering Sea	−0.385	0.489	Coast Redwood
		0.231	Oak
		0.797	Alder
Canonical variate 2			
Subtropical	0.172	0.849	Pine
Transitional	0.101	0.022	Spruce
EBC	0.435	1.034	Western Hemlock
Bering Sea	−0.579	0.096	Coast Redwood
		0.418	Oak
		0.415	Alder

combination of radiolarian assemblages associated with coastal upwelling (increased EBC assemblage) and reduction of the very cold North Pacific water (reduced Bering Sea and Transitional assemblages) with a combination of redwood, western hemlock, and alder pollen (Table 3). The correlation of increased upwelling with this pollen assemblage (Table 3) is reasonable because coastal redwood forests depend on fog, which is associated with summer upwelling. The very high correlation between the marine and continental records on these time scales suggests that the response time of these two systems to climate change is similar. Note the clear presence of an oscillation at Younger Dryas time in the radiolarian variate (Fig. 11), but limited response in the pollen, and the relatively subdued responses in both groups within the glacial period (>15 ka).

The radiolarian and pollen time series for the second canonical variate (which by definition is orthogonal to the first) have a correlation coefficient of 0.60. As shown in Table 3, this variate relates negative contributions of the Bering Sea assemblage and positive contributions of the EBC, subtropical and transitional fauna with increases in western hemlock and pine and to a lesser extent oak and alder. The time series of this variate are

most highly correlated with the western hemlock pollen and transitional faunal records. The time series of the second variate show a long-term trend with higher values between 75,000 and 140,000 cal-years BP as compared to the younger interval 0–75,000 cal-years BP (Fig. 12). This long-term trend is similar to the western hemlock pollen record (compare Figs. 10 and 12). No single radiolarian assemblage shows this trend, but the radiolarian canonical variate faithfully reproduces the pattern observed in the pollen variate and hemlock records. Western Hemlock is in most abundance in the coastal rainforest of western Washington and British Columbia (Fig. 3) just north of the present West Wind Drift (Fig. 1). Thus, we might expect a correlation between the western hemlock pollen and transitional radiolarian fauna. However, the second variate suggests that the general reduction in hemlock pollen at site EW9504A-17PC is also related but in a more complex way to oceanographic changes in the region.

The very high degree of canonical correlation between these two independent data sets suggests that there is a strong link between the continental and ocean response to millennial scale climate change. The relationship between coastal upwelling and coastal redwood forests suggests that this link is more than a simple response to the same climate forcing, but rather changes in oceanographic conditions on these time scales have a direct impact on coastal climates.

4.4. Millennial scale climate variability in the Northeast Pacific

Detailed comparison of the time series from marine cores with those from ice cores such as the GISP2 $\delta^{18}O$ record is hindered by limited precision of the stratigraphic and/or chronologic links. Examination of the time series in our longest and most complete data set, EW9504-17PC, suggests that on wavelengths of about 10 ky (the scale of North Atlantic "Heinrich" Events) the variability is very similar (e.g., compare the Bering Sea, EBC and Transitional assemblage the GISP2 $\delta^{18}O$ in Fig. 7). At shorter wavelengths similar to Dansgaard–Oeschger cycles (wavelength of 1.5 ky; Dansgaard et al., 1993) the amplitudes in the GISP2 $\delta^{18}O$ record are not matched in core EW9504-17PC by the paleoceanographic records nor the pollen time series (Figs. 7 and 10; discussed below).

To provide a framework to allow some detailed analysis of these time series we make the following assumptions: (1) the first canonical variate determined from the marine (Radiolaria) and terrestrial (pollen) climate records represents the best record of climate change in the Northeast Pacific; (2) that this record is highly correlated to the record of North Atlantic climate as represented by the GISP2 $\delta^{18}O$ record and; (3) that based on where we have detailed AMS-^{14}C dates, there is minimal lag between these two climate records (Fig. 11a). The correlation coefficient for the radiolarian first canonical variate time series in core EW9504-17PC and the GISP2 $\delta^{18}O$ record is 0.70. Thus, a detailed chronology for EW9504-17PC can be determined if we assume that the first canonical variate is maximally correlated with the GISP2 $\delta^{18}O$ record.

We used the inverse techniques of Martinson et al. (1982) with 15 mapping coefficients (resolution of less than 20 year wavelengths) to correlate the first radiolarian canonical variate (black curve in Fig. 12) with the smoothed GISP2 $\delta^{18}O$ record. The GISP2 record was low-pass filtered using a bioturbation model similar to that of Peng et al. (1979) and an assumed mixing depth of 8 cm with a diffusivity of 60 cm^2/ky. The bioturbation model was applied to the GISP2 $\delta^{18}O$ record to create what we assume that record would be if measured in a deep-sea sediment core with the same sedimentation rate as EW9504-17PC. This smoothing effectively removed variability at periods shorter than 2.5 ky.

The correlation coefficient after mapping the first canonical variate and the smoothed GISP2 $\delta^{18}O$ record is 0.81. The transitional, EBC, Bering Sea radiolarian assemblages and the western hemlock pollen time series are plotted on this new time scale in Fig. 13. Fig. 13 shows that at wavelengths longer than 3 ky, the amplitudes and wavelength of variability of the paleoclimate records are highly correlated with the ice core isotopic record. Warmer intervals tend to be correlated with enhanced upwelling in the Northeast Pacific and associated pollen response and reduced cold North Pacific water masses (reduced Bering Sea assemblage). Between 25 and 75 ka, warmer intervals also are associated with increases in western hemlock, associated with the moist coastal forests of the Pacific Northwest.

In summary, until a detailed chronostratigraphic framework can be determined we still cannot determine the true dynamics of the linkages between Greenland and the Pacific Northwest. However, where we do have a detailed independent chronology (Fig. 11a), little lag is observed between these records. This observation, combined with the response of the Northeast Pacific to wind-forced upwelling, supports earlier inferences that the linkage between these two regions is through the atmosphere.

4.5. Dansgaard–Oeschger cycles

Dansgaard–Oeschger cycles, first observed in Greenland ice core records (Dansgaard et al., 1993), are clearly seen in paleoceanographic records from within the Santa Barbara Basin (Hendy and Kennett, 2000) and in high sedimentation rate sites off southern California just outside of the Santa Barbara Basin (Kennett et al., 2000). In our most complete and longest data set,

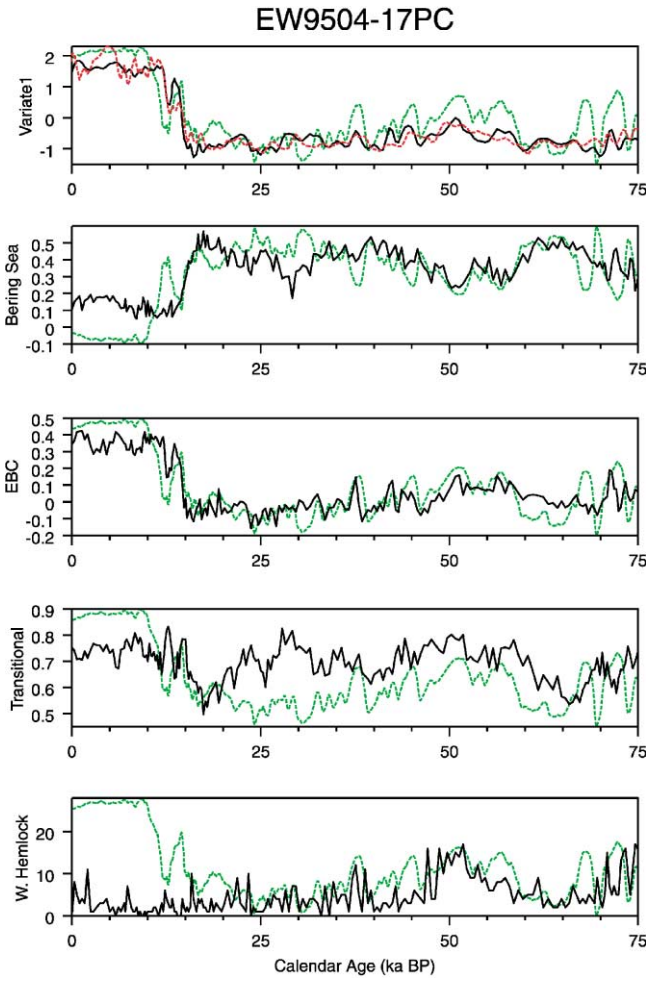

Fig. 13. Time series from EW9504-17PC plotted on a time scale determined from inverse mapping the first radiolarian canonical variate to the GISP2 $\delta^{18}O$. Time series same as shown in Figs. 7, 10 and 12. Green curve is the "bioturbated" (low pass filtered) GISP2 $\delta^{18}O$ record (see text for details).

EW9504-17PC, we do not observe evidence for these cycles. Why? Possible answers include: (1) bioturbation has attenuated cycles at these frequencies (sedimentation rates for the southern California margin sites have sedimentation rates of 20–50 cm/ky compared to sedimentation rates for EW9504-17PC of 10 cm/ky); (2) the 470 year sample resolution is near the limit to resolve these cycles and/or; (3) these events do not strongly affect this site.

We used a bioturbation model based on that of Peng et al. (1979) to evaluate how the bioturbation would modify the GISP2 $\delta^{18}O$ data assuming that this record was contained in a sediment core with the same sampling interval and sedimentation rate as EW9504-17PC. In this model, the bioturbation layers is 10 cm thick. These results suggest that bioturbation may have indeed smoothed the record from core EW9504-17PC sufficiently to remove singles at wavelength similar to the Dansgaard–Oeschger cycles.

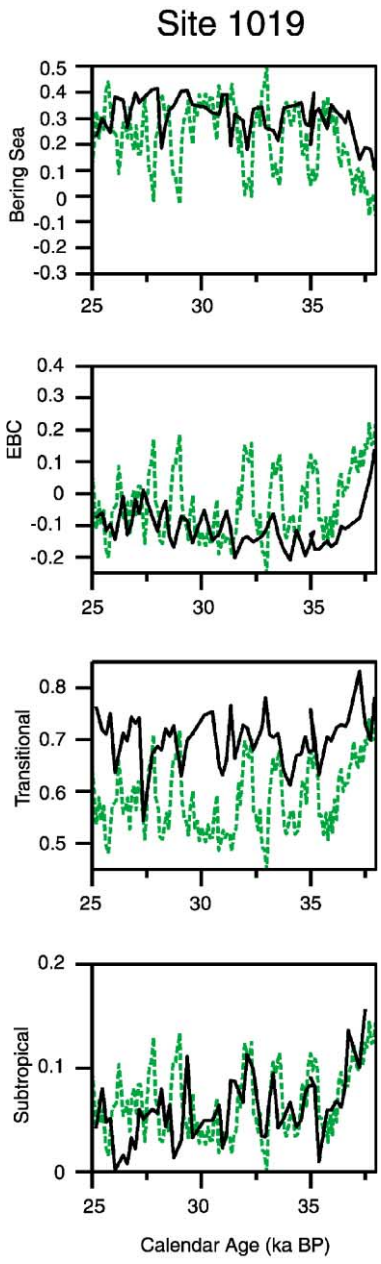

Fig. 14. Selected time series from ODP Site 1019 for the interval 25,000–38,000 cal-years BP. Green curve as in Fig. 4.

Site 1019 has the highest resolution sampling combined with a relatively high sedimentation rate (~38 cm/ky over the interval dated with AMS-^{14}C dates, Table 2). Thus, this site has the potential of preserving Dansgaard–Oeschger cycles. In Fig. 14, we plot the radiolarian assemblages from this site for the interval 25,000–38,000 cal-years BP. Unfortunately, this interval is beyond the available AMS-^{14}C ages for this core so exact correlation to the GISP2 $\delta^{18}O$ data is not possible. In each frame of Fig. 14, the minimum and maximum values for the *y*-axes were determined for the entire interval of the core (0–38,000 cal-years BP). Thus

similar amplitude changes of the radiolarian time series and the GISP2 $\delta^{18}O$ data reflect the same fraction of the full glacial to interglacial change in each time series. Over this interval the amplitude of change in the key assemblages that respond to the millennial scale variability of the region (the Bering Sea and the EBC assemblages) is not as large as the ice core $\delta^{18}O$ data. However, the variability of the Subtropical assemblage resembles the GISP2 $\delta^{18}O$ data (Fig. 14). A similar number of peaks are found in both data sets and the amplitudes of change are very similar. Examination of Fig. 5 shows that the amplitude of the subtropical assemblage at our southern most site, EW9504-13PC, is also similar to the GISP2 $\delta^{18}O$ data. Unfortunately, sample resolution in the interval of 25,000–35,000 cal-years BP is low in core EW9504-13PC because of reduced sedimentation rates during this interval.

Unlike the deglacial response of EW9504-13PC where we see an increase in the Subtropical fauna that is matched by a decrease in other fauna, the changes in the Subtropical fauna shown in Fig. 14 are not matched by changes in the other fauna. Thus, these preliminary data suggest that the response of the Northeast Pacific to climate events on the time scales of Dansgaard–Oeschger cycles may result from variability in the subtropical and/or tropical Pacific. A high resolution study of the paleoceanography of the Santa Barbara Basin also showed that during the Holocene most of the variability in this regions is associated with the subtropical assemblage (Pisias, 1978). From these data Pisias (1978) inferred changes in the northward flow of the Southern California countercurrent.

6. Conclusions

Analysis of radiolarian microfossils, stable isotopes and pollen in sediment cores from the ocean off Northern California and Oregon provides records of surface ocean variability on millennial time scales during the last 150,000 years. Radiolarian based sea-surface temperature estimates suggest changes of the order of 2°C. In coastal waters these temperature changes mainly reflect changes in California Current advection but are moderated by enhanced coastal upwelling during warm intervals. Radiolarian species reflect both processes, suggesting that at least part of the response to Heinrich scale events in the Northeast Pacific is coastal upwelling related to change in atmospheric circulation pattern.

Pollen extracted from these marine sediment cores provides the opportunity to compare directly the climate response of continental and oceanic systems. Canonical correlation reveals significant correlation between the continental and marine records. The first canonical variate ($r = 0.91$) correlates high coastal upwelling with increased redwood and alder pollen. This correlation is reasonable since coastal redwood forests depend on fog, which is associated with summer upwelling. A second canonical variate ($r = 0.60$) relates very cold water with reduced western hemlock pollen abundance.

The paleoclimate records from the Northeast Pacific are correlated to the paleoclimate record of the North Atlantic provided by ice-core $\delta^{18}O$ at wavelengths longer than about 3 kyr. This correlation suggests that warmer events within the last glacial interval are associated with increased coastal upwelling, reduced advection of cold, North Pacific water masses and wetter conditions in the coastal forests of the Pacific Northwest. Available records that resolve Dansgaard–Oeschger cycles suggest that the response of the northeast Pacific to climate events on these time scales reflect variations in the extent of subtropical watermasses.

Our results suggest that Heinrich-scale events (similar to those of the North Atlantic Ocean) and the Dansgaard–Oeschger-scale cycles (similar to those recorded in the Greenland ice-core $\delta^{18}O$ records) are manifested in the Northeast Pacific in very different ways. We speculate that Heinrich-scale variability is transmitted to the Northeast Pacific by an atmospheric response to the partial deflation of the Laurentide ice sheet that has a large, direct effect on mid-latitude atmospheric circulation. On time scales of Dansgaard–Oeschger events, our data suggest that subtropical watermasses are involved with the cycles observed in the Northeast Pacific. Future research will determine if the low-latitudes play a key role in causing these cycles or whether they are involved in transmitting change to the Northeast Pacific from another source.

References

Bakun, A., Nelson, C.A., 1991. The seasonal cycle of wind-stress curl in subtropical eastern boundary current regions. Journal of Physical Oceanography 21, 1815–1834.

Barbour, M.G., Billings, W.D., 1988. North American Terrestrial Vegetation. Cambridge University Press, Cambridge.

Barbour, M.G., Major, J., 1977. Terrestrial Vegetation of California. Wiley, New York.

Cochran, W.G., 1963. Sampling Techniques, Wiley, New York, 413p.

Climate: Long-Range Investigation, Mapping and Prediction (CLIMAP) Project Members, 1981. Seasonal reconstructions of the Earth's surface at the last glacial maximum, Geological Society of America Map Chart Series. MC-36.

Dansgaard, W., et al., 1993. Evidence for general instability of the past climate from 250-kyr ice-core record. Nature 364, 218–220.

Elford, C.R., 1974. The climate of California. In: van der Leeden, F., Troise, F.L. (Eds.), Climates of the States. Water Information Center, Port Washington, NY, pp. 538–594.

Grigg, L.D., Whitlock, C., 1998. Late-glacial vegetation and climate change in western Oregon. Quaternary Research 49, 287–298.

Heine, J.T., 1998. Extent, timing, and climate implications of glacier advances near Mount Rainier, Washington, USA, at the Pleistocene/Holocene transition. Quaternary Science Reviews 17, 1139–1148.

Hendy, I.L., Kennett, J.P., 2000. Dansgaard–Oeschger cycles and the california current system: planktonic foraminiferal response to rapid climate change in Santa Barbara Basin, Ocean Drilling Program Hole 893A. Paleoceanography 15, 30–42.

Heusser, L., 1998. Direct correlation of millennial-scale changes in western North American vegetation and climate with changes in the California Current system over the past ~60 kyr. Paleoceanography 13 (3), 252–262.

Heusser, L., Balsam, W.L., 1977. Pollen distribution in the Northeast Pacific Ocean. Quaternary Research 7, 45–62.

Heusser, L.E., Stock, C.E., 1984. Preparation techniques for concentrating pollen from marine sediments and other sediments with low pollen density. Palynology 8, 225–227.

Heusser, L., Lyle, M., Mix, A., 2000. Vegetation and climate of the northwest coast of North America during the last 500 ky. High-resolution pollen evidence from the northern California Margin. In: Lyle, M., Koizumi, I., Richter, C. (Eds.), Proceedings ODP 167: College Station, TX (Ocean Drilling Program), pp. 217–226.

Hitchcock, C.L., Cronquist, A., 1973. Flora of the Pacific Northwest. University of Washington Press, Seattle.

Hood, R.R., Abbott, M.R., Huyer, A., Kosro, P.M., 1994. Surface patterns in temperature, flow, phytoplankton biomass, and species composition in the coastal transition zone of northern California. Journal of Geophysical Research 95, 18081–18094.

Hostetler, S.W., Clark, P.U., Bartlein, P.J., Mix, A.C., Pisias, N.G., 1999. Atmospheric transmission of North Atlantic Heinrich events. Journal of Geophysical Research 104, 3947–3952.

Huyer, A., 1983. Coastal upwelling in the California Current System. Progress in Oceanography 12, 259–284.

Imbrie, J., Kipp, N.G., 1971. A new micropaleontological method for quantitative paleoclimatology: application to a late Pleistocene Caribbean core. In: Turekian, K. (Ed.), Late Cenozoic Glacial Ages. Yale University Press, New Haven, CT, pp. 71–181.

Kennett, J.P., Roark, E.B., Cannariato, K.G., Ingram, B.L., Tada, R., 2000. Latest Quaternary paleclimatic and radiocarbon chronology, Hole 1017E, southern California margin, In: Lyle, M., Koizumi, I., Richter, C., Moore Jr., T.C. (Eds.), Proceedings ODP, Sci., Results, 167: College Station TX (Ocean Drilling Program), pp. 249–254.

Levitus, S., 1982. Climatological Atlas of the World. Rockville Md: NOAA Professional Paper 13. 173.

Martinson, D.G., Menke, W., Stoffa, P., 1982. An inverse approach to signal correlation. Journal of Geophysical Research 87, 4807–4818.

Miller, C.B., Frost, B.W., Booth, B., Wheeler, P.A., Landry, M.R., Welschmeyer, N., 1991. Ecological processes in the Subarctic Pacific: iron limitation cannot be the whole story. Oceanography 4, 71–78.

Mix, A.C., Lund, D.C., Pisias, N.G., Boden, P., Bornmalm, L., Lyle, M., Pike, J., 1999. Rapid climate oscillations in the Northeast Pacific during the last deglaciation reflect northern and southern hemisphere sources. In: Clark, P.U., Webb, R., Keigwin, L. (Eds.), Mechanisms of Global Climate Change at Millennial Time Scales, Geophysical Monograph 112, pp. 127–148.

Munz, P.A., 1968. A California Flora. Berkeley, CA: University of California Press.

Ortiz, J.D., Mix, A.C., Collier, R.W., 1995. Environmental control of living symbiotic and asymbiotic foraminifera of the California Current. Paleoceanography 10 (6), 987–1010.

Ortiz, J.D., Mix, A.C., Hostetler, S., Kashgarian, M., 1997. The California Current of the last glacial maximum: reconstruction at 42°N based on multiple proxies. Paleoceanography 12 (2), 191–206.

Peng, T.-H., Broekcer, W.S., Berger, W.H., 1979. Rates of benthic mixing in deep-sea sediments as determined by radioactive tracers. Quaternary Research 11, 141–149.

Pisias, N.G., 1978. Paleoceanography of the Santa Barbara Basin during the last 8000 years. Quaternary Research 10, 366–384.

Pisias, N.G., Roelofs, A., Weber, M., 1997. Radiolarian-based transfer function for estimating mean surface ocean temperatures and seasonal range. Paleoceanography 12 (3), 365–379.

Prahl, F.G., Pisias, N.G., Sabin, A.L., Sparrow, M., 1995. Assessment of sea surface temperature at 42°N in the California Current System over the last 300,000 years. Paleoceanography 10 (4), 763–774.

Roden, G.I., 1975. On North Pacific temperature, salinity, sound velocity, and density fronts and their relation to the wind and energy flux fields. Journal of Physical Oceanography 5, 557–571.

Roelofs, A.K., Pisias, N.G., 1986. Revised technique for preparing quantitative radiolarian slides from deep-sea sediments. Micropaleontology 24, 182–185.

Sabin, A.L., Pisias, N.G., 1996. Sea surface temperature changes in the northeast Pacific during the past 20,000 years and their relationship to climate change in northwestern North America. Quaternary Research 46, 48–61.

Stuiver, M., Grootes, P.M., 2000. GISP2 oxygen isotope ratios. Quaternary Research 53, 277–284.

Stuiver, M., Reimer, P.J., Bard, E., Beck, J.W., Burr, G.S., Hughen, K.A., Kromer, B., McCormac, F.G., vanderPlicht, J., Spurk, M., 1998. INTCAL98 radiocarbon age calibration 24,000–0 cal BP. Radiocarbon 40, 1041–1083.

Welling, L.A., Pisias, N.G., Roelofs, A.K., 1992. Radiolarian microfauna in the northern California Current System: indicators of mulitple processes controlling productivity. In: Summerhayes, C.P., W.L. Prell, K.C. Emeis (Eds.), Upwelling Systems: Evolution Since the Early Miocene, Geol. Soc. Spec. Pub. No. 64, pp. 177–195.

Whitlock, C., Grigg, L.D. 1999. Paleoecological evidence of Milankovitch and sub-Milankovitch climate variations in the western US during the late Quaternary. In: Webb, R.S., Clark, P.U., Keigwin, L.D. (Eds.), The Roles of High and Low Latitudes in Millennial-scale Global Climate Change, AGU, Monograph 112, pp. 227–243.

Whitlock, C., Bartlein, P., 1997. Vegetation and climate change in northwest America during the past 125 kyr. Nature 388, 57–61.